AMERICAN SOCIETY FOR MICROBIOLOGY | Journal of Bacteriology

Fitness benefits of a synonymous substitution in an ancient EF-Tu gene depend on the genetic background

Kaitlyn M. McGrath,[1,2,3] Steven J. Russell,[1] Evrim Fer,[1,4] Eva Garmendia,[5] Ali Hosgel,[1] David A. Baltrus,[3] Betül Kaçar[1]

AUTHOR AFFILIATIONS See affiliation list on p. 13.

ABSTRACT Synonymous mutations are changes to DNA sequence, which occur within translated genes but which do not affect the protein sequence. Although often referred to as silent mutations, evidence suggests that synonymous mutations can affect gene expression, mRNA stability, and even translation efficiency. A collection of both experimental and bioinformatic data has shown that synonymous mutations can impact cell phenotype, yet less is known about the molecular mechanisms and potential of beneficial or adaptive effects of such changes within evolved populations. Here, we report a beneficial synonymous mutation acquired via experimental evolution in an essential gene variant encoding the translation elongation factor protein EF-Tu. We demonstrate that this particular synonymous mutation increases EF-Tu mRNA and protein levels as well as global polysome abundance on RNA transcripts. Although presence of the synonymous mutation is clearly causative of such changes, we also demonstrate that fitness benefits are highly contingent on other potentiating mutations present within the genetic background in which the mutation arose. Our results underscore the importance of beneficial synonymous mutations, especially those that affect levels of proteins that are key for cellular processes.

IMPORTANCE This study explores the degree to which synonymous mutations in essential genes can influence adaptation in bacteria. An experimental system whereby an *Escherichia coli* strain harboring an engineered translation protein elongation factor-Tu (EF-Tu) was subjected to laboratory evolution. We find that a synonymous mutation acquired on the gene encoding for EF-Tu is conditionally beneficial for bacterial fitness. Our findings provide insight into the importance of the genetic background when a synonymous substitution is favored by natural selection and how such changes have the potential to impact evolution when critical cellular processes are involved.

KEYWORDS translation, elongation factor EF-Tu, synonymous mutation, experimental evolution

Synonymous mutations are changes in the codon sequence, which do not alter the sequence of the translated peptide. While often considered neutral or silent, evidence suggests that synonymous mutations can affect cellular phenotypes and potentially impact population growth fitness (1–10) as well as gene and protein expression. For example, synonymous mutations may cause modification of mRNA levels by enhancing promoters (8) and altering mRNA folding and/or stability (10–13). Furthermore, changes in mRNA secondary structure can interfere with protein synthesis, disrupting translation speed and accuracy (10, 14–17), which can ultimately impact protein levels. Since translation coincides with protein folding, changes in translation speed and accuracy can influence both protein expression and function (18).

Codon bias refers to the uneven distribution of synonymous codons for the same amino acid in a gene or genome (19). Given the importance of mRNA stability and

Editor Tina M. Henkin, Ohio State University, Columbus, Ohio, USA

Address correspondence to Betül Kaçar, bkacar@wisc.edu.

The authors declare no conflict of interest.

See the funding table on p. 13.

Received 2 October 2023
Accepted 5 January 2024
Published 30 January 2024

translation rate for cellular functions, the use of synonymous codons has the potential to impact fitness in a variety of ways. However, the impact of codon bias on translation speed, accuracy, and efficiency is not yet clear. Studies have correlated highly expressed genes with high levels of codon bias which may provide an advantage for cellular fitness (16, 19–23). Conversely, some studies suggest that codon bias has minimal or no effect on fitness (24–26), while others show examples of beneficial synonymous mutations with less-preferred codons (6). Taken together, little is known about the molecular mechanisms and potential of beneficial or adaptive fitness effects of such changes within evolved populations.

In this study, we explored the degree in which a key synonymous mutation influences essential gene adaptation in bacteria building on an experimental system whereby an *Escherichia coli* (*E. coli*) strain harboring an engineered essential gene was subjected to laboratory evolution (27). Specifically, an essential protein in translation, elongation factor Tu (EF-Tu), was directly replaced with a phylogenetically inferred ancestor, AnEF, leading to a fitness decrease of the engineered strain (27, 28). EF-Tu is an essential GTPase that binds to amino-acylated tRNAs and shuttles them to the A-site of the ribosome (Fig. 1A) (29). EF-Tu is critical in mediating the rate and accuracy of translation elongation (30) and is one of the most abundant proteins in the cell, making up ~6% of the total protein in *E. coli* (31, 32).

We report a single synonymous mutation discovered in the *anEF* gene coding region in one of the experimentally evolved engineered *E. coli* populations. Whole genome sequencing reveals that the synonymous mutation in *anEF* appears after generation 2,000 and sweeps to fixation within the population by the 2,500th generation. Genetic and cellular analyses demonstrate that this synonymous mutation is beneficial during laboratory growth and increases the mRNA and protein levels of AnEF, yet these fitness effects are contingent on the presence of one or more additional mutations in the evolved genetic background. Furthermore, we show that this synonymous mutation increases the abundance of polysomes during translation. Our results demonstrate that synonymous mutations may play a key role when affecting the levels of proteins that limit key cellular processes.

RESULTS

In previous work, we engineered and experimentally evolved an *E. coli* strain widely used for laboratory evolution studies, REL606, to replace a single copy of ancestral EF-Tu by substituting the *tufB* gene with an inferred ancestral allele in a strain where the homologous gene copy *tufA* was deleted (*ΔtufA*, *tufB::anEF*) (27). We refer to *ΔtufA tufB::anEF* as the ancestor strain hereafter (Table 1). *E. coli*'s EF-Tu and AnEF share ~95% protein sequence identity (Fig. S1). Additionally, the predicted structure of AnEF exhibits a root mean square deviation (RMSD) value of 1.63 Å when overlaid with *E. coli* EF-Tu (33) (Fig. 1B).

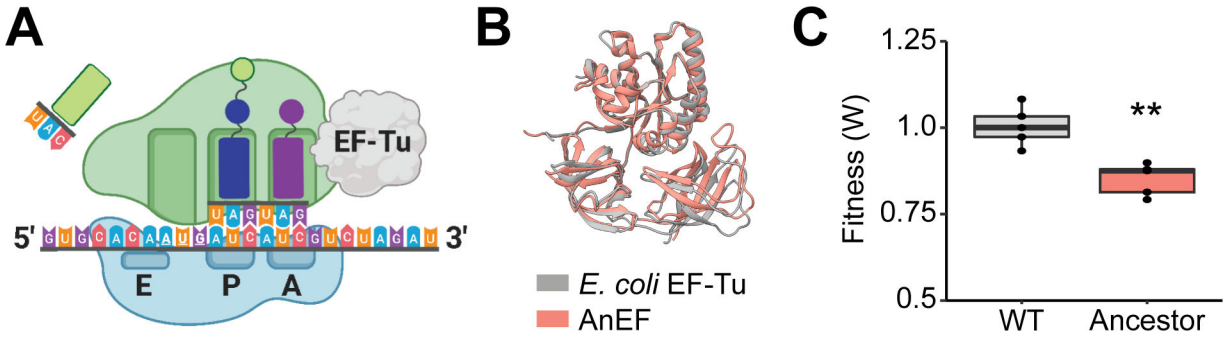

FIG 1 Replacement of EF-Tu with ancestral EF-Tu (AnEF). (A) Overall schematic of interaction between *E. coli* EF-Tu and ribosome. (B) Overlay of *E. coli* EF-Tu (PDB: 5AFI) and AnEF predicted structures (root mean square deviation, 1.63 Å). (C) Competitive fitness of the REL606 harboring AnEF (ancestor) relative to the REL606 Δ*tufA* (wild type), *t*-test ($n = 5$).

TABLE 1 List of *E. coli* samples used in the study[a]

Samples	Genotype and relevant characteristics
Ancestor	REL606 Δ*tufA*, *tufB*::*anEF*
g500	REL606 Δ*tufA*, *tufB*::*anEF*, 500 generations
g1000	REL606 Δ*tufA*, *tufB*::*anEF*, evolved 1,000 generations
g1500	REL606 Δ*tufA*, *tufB*::*anEF*, evolved 1,500 generations
g2000	REL606 Δ*tufA*, *tufB*::*anEF*, evolved 2,000 generations
g2500	REL606 Δ*tufA*, *tufB*::*anEF*, evolved 2,500 generations
g3000	REL606 Δ*tufA*, *tufB*::*anEF*, evolved 3,000 generations
Evolved ($AnEF_{C45T}$) (isolated clone)	REL606 Δ*tufA*, *tufB*::*anEF*, evolved 3,000 generations, *anEF* C45T (GTC→GTT)
Evolved ($AnEF_{T45C}$) (engineered strain)	REL606 Δ*tufA*, *tufB*::*anEF*, evolved 3,000 generations, *anEF* T45C (GTT→GTC)
Ancestor ($AnEF_{C45T}$) (engineered strain)	REL606 Δ*tufA*, *tufB*::*anEF* C45T (GTC→GTT)

[a]Bacterial strain or population name and characteristics are indicated. A complete list of constructs used for genome engineering can be found under Supplementary Information.

We assessed the effect of AnEF allele replacement into *E. coli* in glucose minimal medium via co-culture competition and compared its fitness with a wild-type strain containing a single copy of the wild-type EF-Tu (*E. coli* REL606 Δ*tufA*). The relative fitness of the modified ancestor strain was ~0.87 [$n = 5$, $P < 0.01$, analysis of variance (ANOVA)] (Fig. 1C). Eight lineages propagated from a single colony of REL606 *ΔtufA, tufB::anEF* was then subjected to 3,000 generations of laboratory evolution through serial propagation of bacterial populations (Fig. 2A) (34). An *E. coli* REL606 Δ*tufA* strain was evolved in parallel as a control. Using co-culture competition assays, we quantified the fitness of the evolved population relative to the ancestor strain every 1,000 generations of the evolution experiment (Fig 2B). Genomes of evolved populations were sequenced at six different time points: generations 500, 1,000, 1,500, 2,000, 2,500, and 3,000.

Population sequencing of one particular lineage reveals a "fixed" (reached a frequency of 100% in the population) synonymous mutation in the ancient EF-Tu gene coding region in generation 2,500. In this lineage, generation 500 had three fixed nonsynonymous mutations in genes *ydjN* and *fadA* and a genomic deletion in the *rbs* operon (*rbsD*-[*rbsR*]) (Fig. 2C and D; Table S3). Generations 1,000 to 2,000 acquired three additional fixed nonsynonymous mutations in genes *mrdA*, *ydfI*, and *yfaS* (Fig. 2C; Table S3). Finally, in generations 2,500 and 3,000, we identified two more fixed mutations, a non-synonymous mutation in gene *pykF* and a synonymous mutation in the replaced gene *anEF* (Fig. 2C; Table S3). Substitution dynamics reconstruction associated with each generation time point (Fig. 2D) shows that nonsynonymous mutations arose independently in four other genes *ECB_01992* (arose in generation 1,000), *hupA* (generation 1,500), *caiD* (generation 1,500), and *hslU* (generation 2,000) (Fig. 2D). However, these mutations did not reach fixation and, instead, were eventually lost from the population. The patterns we observed in genotype dynamics is consistent with each detected fixed mutation (Fig. 2C).

The rise and effect of the AnEF synonymous mutation

Intriguingly, at generation 2,500, a synonymous mutation appeared in the *anEF* gene coding region, in one out of eight parallel evolved lineages. Notably, the synonymous mutation reached 100% fixation rapidly, appearing between generations 2,000 and 2,500 (Fig. 2C and D; Table S3) and, ultimately, swept the entire population by generation 2,500 (Fig. 2D). Specifically, we identified a C > T mutation at nucleotide 45, GTC (Val)→GTT (Val) mutation, in the N-terminal coding region of the *anEF* gene (Fig. 3A; Table 1). The presence of the mutation at each generation was successfully verified with whole genome sequencing (Fig. 2C and D; Table S3).

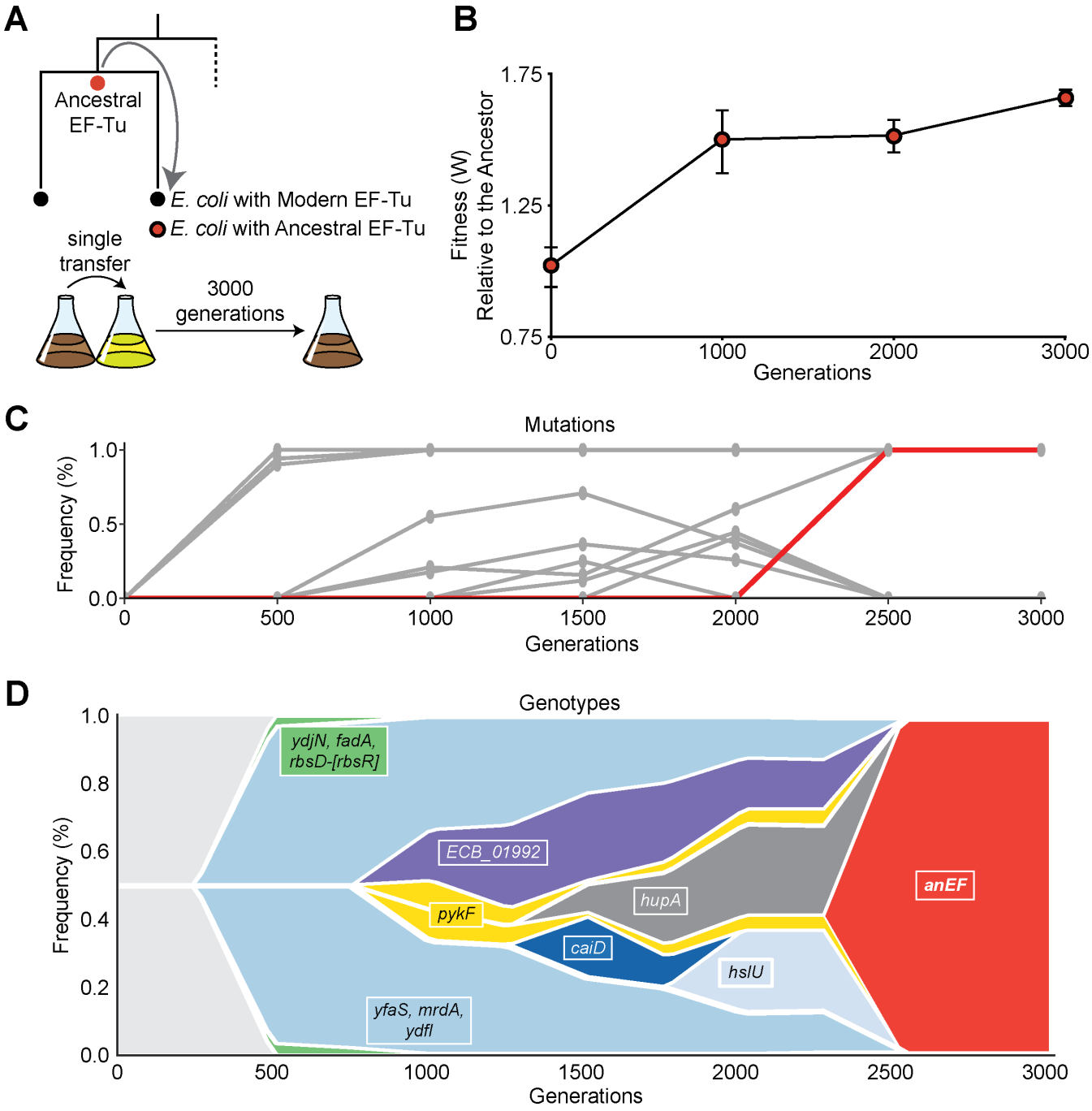

FIG 2 Evolutionary dynamics of an *E. coli* strain harboring an ancestral EF-Tu gene. (A) Engineering and evolution experiment schematics. (B) Change in fitness of evolved population relative to the ancestor. (C) Gene mutation frequencies in evolved population over 3,000 generations. *anEF* gene synonymous mutation highlighted in red. (D) Muller plot demonstrating the genotype dynamics across laboratory evolution with 3,000 generations. Plotted are the mutations in genes that reached a minimum frequency of 25%, and highlighted in red is the selection frequency of the *anEF* synonymous mutation.

We hypothesized that if the synonymous mutation is beneficial, reverting the evolved mutation in the *anEF* gene back to the ancestral nucleotide would negatively affect fitness. To test this hypothesis, we engineered the codon containing the synonymous mutation back to the ancestral codon sequence while keeping the rest of the genetic background (including all other fixed mutations) constant. This new strain is referred to as evolved + $AnEF_{T45C}$ (Table 1). Furthermore, to test if the fitness impact of the synonymous mutation was background dependent, we introduced the synonymous mutation

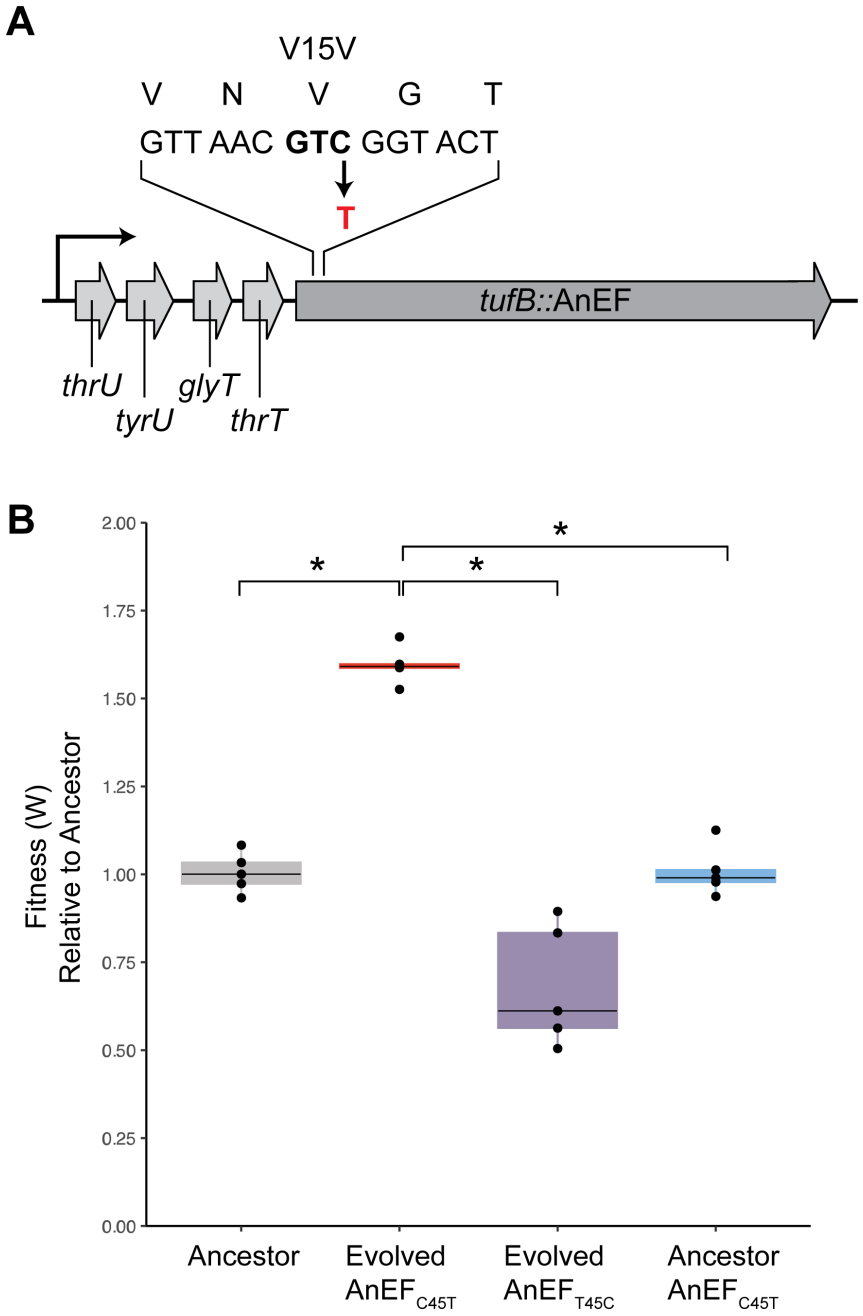

FIG 3 Fitness and growth characteristics of $AnEF_{C45T}$. (A) Schematic of $AnEF_{C45T}$. (B) Fitness phenotype between endogenous and isogenic constructs ($n = 5$, ANOVA, Tukey's HSD).

(C45T) into the *anEF* unevolved allele in the ancestral background (referred to as ancestor + $AnEF_{C45T}$) (Table 1; Materials and Methods). All isogenic constructs were confirmed via local DNA sequencing and whole genome sequencing.

The synonymous mutation is conditionally beneficial depending on the genetic background

We next measured the impact of the C45T synonymous mutation on organismal fitness via co-culture competition assays by calculating relative fitness (W). In agreement with the previously published studies, the replacement of native *E. coli* EF-Tu with the ancestral EF-Tu AnEF causes a 13% decrease in fitness ($W = 0.87$, $P < 0.01$, ANOVA Tukey's

Honestly Significant Difference, HSD) (Fig. 1C) (27, 28), which upon 3,000 generations of laboratory evolution is recovered and increased by 60% relative to the ancestor (evolved $AnEF_{C45T}$, W = 1.6, $P < 0.01$, ANOVA Tukey's HSD) (Fig. 3B). Substitution of the synonymous mutation with the native codon significantly decreases the fitness of the evolved microbe by 30% (evolved $AnEF_{T45C}$, W = 0.7, $P < 0.01$, ANOVA Tukey's HSD), whereas introducing the synonymous mutation in the ancestral background has no relative fitness benefit (ancestral $AnEF_{C45T}$, W = 1.00, $P = 0.80$, ANOVA Tukey's HSD) (Fig. 3B). These results show the strong epistasis between the synonymous mutation and the evolved background, demonstrating that the fitness effect of the synonymous mutation depends on the genetic background.

$AnEF_{C45T}$ synonymous mutation is associated with increased mRNA and protein levels

Previous studies have reported that synonymous mutations can impact mRNA and protein levels (6–10). To assess the change in transcript level, we measured mRNA levels via quantitative polymerase chain reaction (qPCR) and calculated ΔΔCq values to compare AnEF mRNA with and without the evolved synonymous mutation ($n = 3$). Relative to the ancestor, we observed a threefold increase in the evolved strain ($P < 0.05$, *t*-test) and a two-fold increase in the ancestor with the synonymous mutation (ancestor + $AnEF_{C45T}$, $P < 0.05$, *t*-test) (Fig. 4A; Fig. S2). The mRNA levels of the evolved strain with the synonymous mutation reverted back to the ancestral nucleotide (evolved + $AnEF_{T45C}$) displayed a 30% decrease in AnEF mRNA relative to the ancestor; however, this observation was not significant ($P = 0.06$, *t*-test) (Fig. 4A; Fig. S2). Furthermore, we assessed whether the C45T synonymous mutation has changed the protein levels relative to the ancestor strain ($n = 3$) (Fig. 4B; Fig. S3). AnEF protein levels increase 32.2% in the evolved strain with the C45T synonymous mutation ($P < 0.01$, *t*-test; Materials and Methods) (Fig. 4B; Fig. S2). Similarly, the engineered ancestor with the $AnEF_{C45T}$ allele exhibits a 34.2% increase in AnEF protein levels ($P < 0.01$, *t*-test) (Fig. 4B; Fig. S2). Interestingly, reversion of the synonymous mutation back to the ancestral nucleotide in evolved strain (evolved + $AnEF_{T45C}$) leads to a 15.3% decrease in AnEF protein levels ($P < 0.01$, *t*-test) (Fig. 4B; Fig. S2). Taken together, these data suggest that the evolved

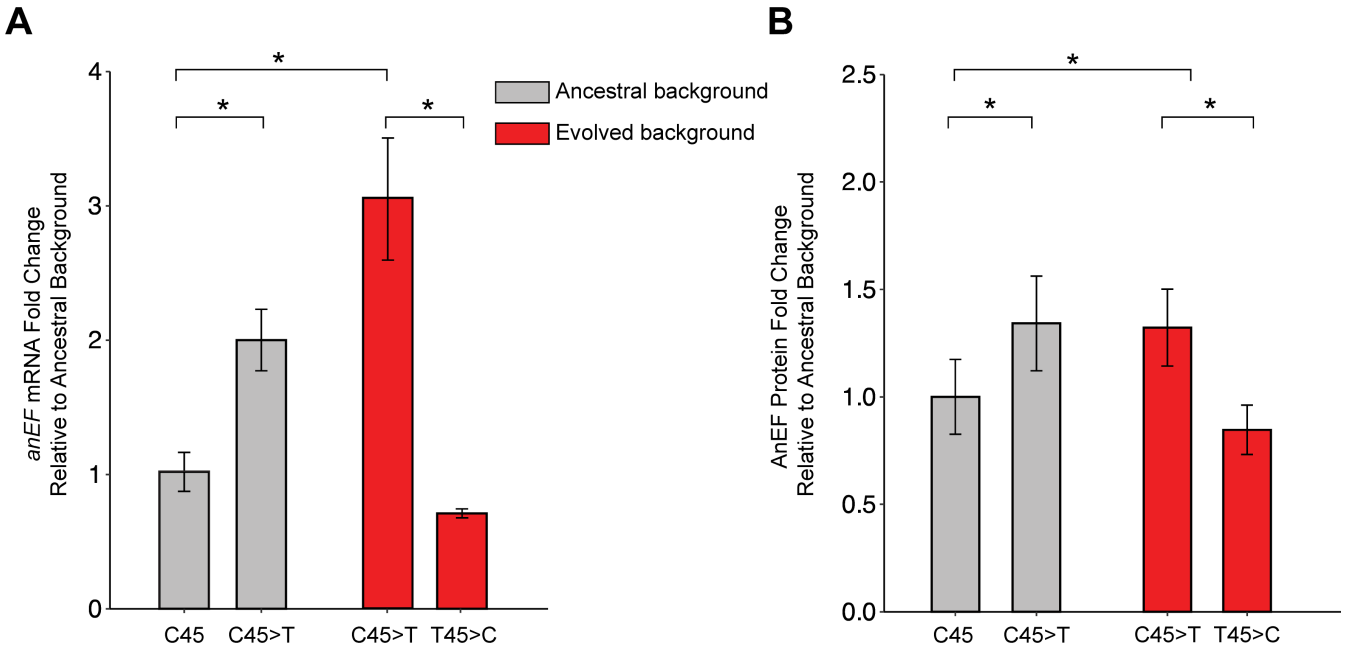

FIG 4 $AnEF_{C45T}$ synonymous mutation detected in the evolved lineage is associated with increased AnEF protein and mRNA levels. (A) qPCR quantification of AnEF mRNA between constructs ($n = 3$, *t*-test). (B) Western blot quantification of AnEF protein between endogenous and isogenic constructs ($n = 3$, *t*-test).

synonymous mutation in AnEF is correlated with an overall increase in AnEF mRNA and protein levels in both the ancestor and evolved genetic backgrounds.

The presence of the synonymous mutation in AnEF leads to an increase in ribosomal abundance in translation elongation

Various studies have demonstrated the link between bacterial growth and ribosomal abundance, showing that growth (and death) rate of bacterial populations is affected by the number of ribosomes (35–38). Elongation factor proteins are highly expressed in the cell (39) and fulfill a crucial role in the ribosome (40). Thus, upon determining the significant impact the synonymous mutation has on AnEF mRNA and protein levels, we asked if the synonymous mutation affects ribosomal abundance. We hypothesized that the evolved strain with the synonymous mutation would exhibit greater number of ribosomes as it displays an increase in population growth fitness, gene, and protein expression.

We inferred the cellular translatome, which refers to all mRNAs associated with ribosomes in protein synthesis, using polysome profiling to assess the impact the AnEF synonymous mutation has on translation. The translation process is made up of four main steps: initiation, elongation, termination, and recycling, where initiation is the assembly and preparation of the ribosome on a transcript and elongation is the decoding process of protein synthesis (41, 42). Polysome profiling provides insight into the translation process by first separating ribosomes via RNA sedimentation and then providing comparative ribosomal abundance for each step of protein synthesis for the corresponding strain. We first assessed the polysome profile of the wild-type REL606 strain (n = 3). As shown in Fig. 5, we used a 10%–40% sucrose gradient for sufficient separation of RNA molecules, of which free RNAs (mRNA, tRNA, etc.) are the lightest and, therefore, will sediment toward the top of the gradient and the heaviest RNA molecules being the longer stretch of polysomes actively translating along an mRNA transcript. Therefore, the first peak detected on a polysome profiles represents the free RNAs in a cell, followed by peaks associated with the small and large ribosomal subunits, 30S and 50S, respectively. The highest peak shown here represents the assembled 70S monosome, which is a single ribosome on an mRNA transcript, or a ribosome in the initiation phase of translation. Finally, each peak following the monosome represents

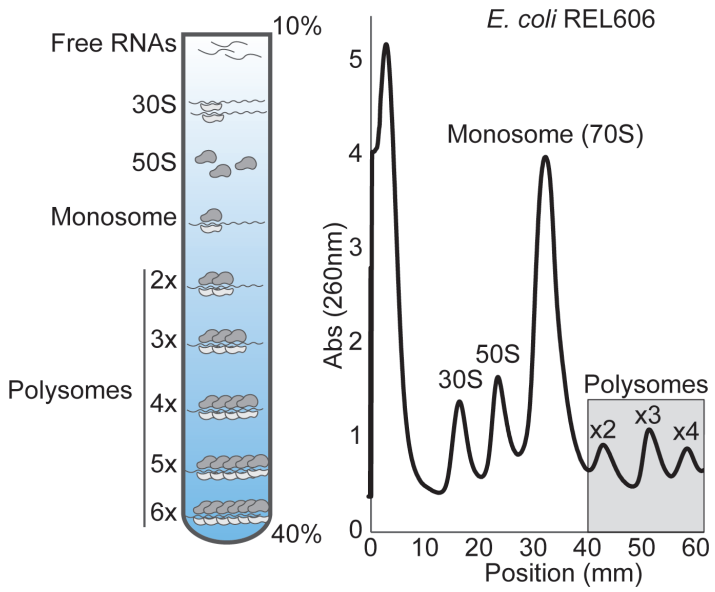

FIG 5 *E. coli* translatome of REL606 assessed via polysome profiling, showing ribosomal abundance measured by 260-nm absorbance along a 10%–40% sucrose gradient (n = 3, t-test).

the stretch of polysomes in the elongation phase of translation (Fig. 5; Materials and Methods).

To assess the impact the AnEF synonymous mutation has on translation, we globally quantified the abundance of ribosome footprints by calculating the area under the curve (AUC) for each ribosomal peak and compared relative ribosomal abundance between the endogenous and isogenic strains ($n = 6$) (Fig. 6; Materials and Methods). Relative to the ancestor, the evolved strain has increased levels of the 30S (~20%, $P = 0.0067$, two-tailed *t*-test) and 50S (~13%, $P = 0.044$, two-tailed *t*-test) ribosomal subunits and a trending increase in the overall polysome abundance (~10%, $P = 0.085$, two-tailed *t*-test) (Fig. 6; Fig. S4). However, compared to ancestor, the evolved strain has decreased levels of 70S monosomes (~17%, $P = 0.0002$, two-tailed *t*-test) (Fig. 6A; Fig. S3).

DISCUSSION

Prior studies demonstrate that *E. coli* can respond to EF-Tu gene perturbations in multiple, contingent ways. For example, a previous study experimentally evolved multiple parallel populations of *E. coli* harboring an ancient EF-Tu gene for over 3,000 generations and reported that the majority of the populations had gained mutations in the promoter region of the EF-Tu gene, resulting in an increase of protein expression (27). Overexpressing the AnEF partially increases *E. coli* fitness (28), demonstrating that fitness may be restricted by the availability of key enzymes that mediate critical cellular processes. Subsequent studies have replaced EF-Tu with several of its extant and extinct orthologs, demonstrating evolutionary distance, together with horizontal gene transfer constraints genomic compatibility and interchangeability (28). Successive generations of synthetic laboratory evolution of EF-Tu variant-harboring strains in different growth conditions were tracked for fitness and mutation accumulations in sweep populations (43). These results demonstrated that there is a measurable negative correlation between the rate of beneficial mutation accumulation and fitness advantage in the translation module, and due to this stalling effect, the translation module could not reach an optimal fitness peak. Even under the most controlled circumstances, it is difficult to predict which array of responses a system will take.

We suggest that when protein levels are the limitation for cell growth, synonymous mutations that increase protein levels may lead to beneficial and adaptive outcomes.

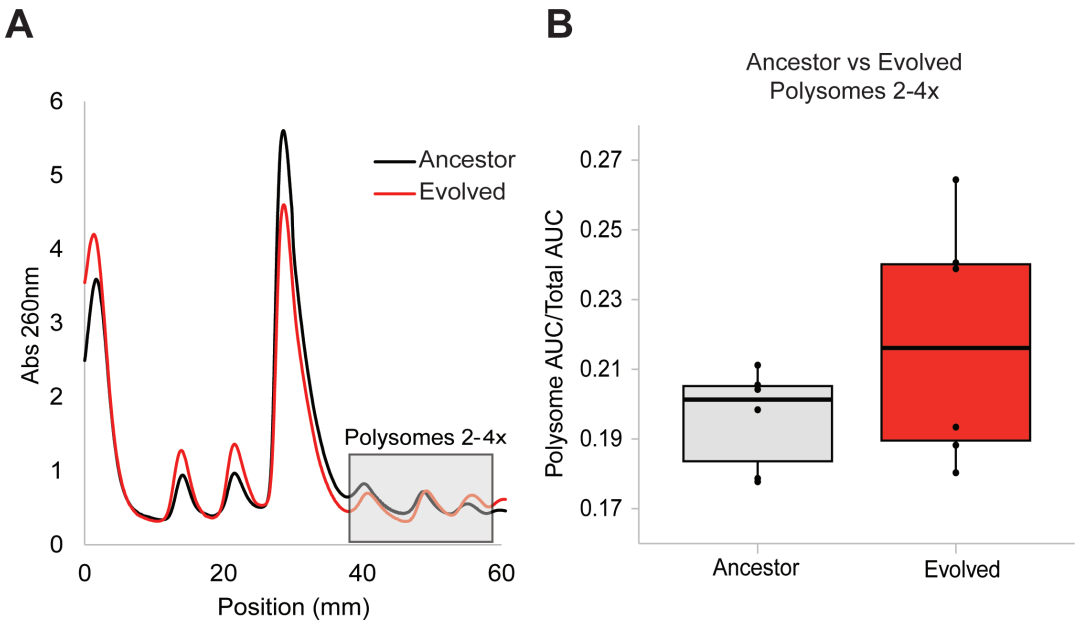

FIG 6 Polysome profiling of the evolved strain (red) relative to the ancestor (black). (B) Quantification of polysome abundance from shaded box in the profiles in generated panel A ($n = 6$, *t*-test).

Indeed, previous laboratory passage studies have reported that synonymous mutations directly influence growth as a result of increased mRNA and protein levels for proteins that sit at bottlenecks in pathways contributing to flux through metabolic systems (6, 44, 45). While these previous studies demonstrate that the amount of the protein available in the system impacts substrate turnover at key nodes in pathways, our study differs in that the amount of the focal protein directly impacts overall cellular translation rate, thus generally influencing the translation rate of all proteins. Although translation can be sustained in *E. coli* by the reconstructed ancient allele of EF-Tu (AnEF), this interchange leads to a decrease in cellular protein synthesis and population fitness. (Fig. 4).

Intriguingly, a previous study identified that the first 65 codons of *tufB* are important for *tufB* regulation in *Salmonella* and that various synonymous mutations near the start codon (including C45) promote an open conformation of the *tufB* mRNA, which leads to increased EF-Tu expression (46). Since AnEF was inserted in place of *tufB* and shares a nucleotide sequence identity of 87%, it is possible that the observed increase in AnEF mRNA and protein levels can thus be explained by the favored open conformation of AnEF mRNA secondary structure. The resulting $anEF_{C45T}$ mRNA sequence between regions −73 and +96 exhibits an unaltered secondary structure when compared to *E. coli tufB* (Fig. S4; Materials and Methods). Moreover, the wild-type *E. coli tufB* codon for valine (position 45) is GTC, which is reported at a frequency of 13.5% in codon usage bias frequency index (47). Interestingly, the synonymous mutation in AnEF changed the codon from GTC to GTT, which is reported at a higher frequency of 39.8%, the second most frequent codon used for valine in *E. coli* for highly expressed genes (47). To what degree this conversion may be attributable to the codon bias requires further mechanistic investigation.

The synonymous mutation detected in AnEF indicates a trending increase in polysome abundance (Fig. 6; Fig. S3), defined by an increase in the number of elongating ribosomes on global mRNA transcripts. Based on this, we develop three scenarios to interpret our results: (i) The increase in polysomes may reflect the observed increase in AnEF protein levels. The transition of translation initiation to elongation is marked by the first translocation via EF-G (41, 42), which is dependent on EF-Tu for bringing a cognate amino-acylated tRNA to form the first dipeptide bond (41, 42). (ii) The increase in polysomes may be due to a decline in translation elongation rate in agreement with the previous studies showing that protein synthesis rate is reduced when translation is dependent on the EF-Tu ancestral variant (28). Furthermore, ancient EF-Tu variants were shown to exhibit significantly low K_M values for dipeptide formation (48), indicating that ancestral EF-Tus are less efficient at sequestering cognate amino-acylated tRNAs to the ribosome. Altogether, ancient EF variant's reduced efficiency at sequestering cognate amino-acylated tRNAs to the ribosome leads to ribosomal stalling in the decoding process (48). Such stalling increases the presence of elongating ribosomes. (iii) Finally, a combinatorial effect of the scenarios (i) and (ii) collectively increases cellular translation behavior. While the boost in AnEF protein amount would not necessarily boost the efficiency of the AnEF function, it would equate to an increase in EF-Tu availability for ribosomes transitioning from translation initiation to elongation. In sum, the increase in polysome abundance on global mRNA transcripts is very likely due to cumulative effects of the increase in AnEF protein amount coupled and the AnEF's kinetic reduction in translation efficiency relative to its extant counterpart.

The AnEF synonymous mutation ($AnEF_{C45T}$) is the cause for the beneficial changes, yet the advantageous impact of the mutation on the population fitness is observed only when the synonymous mutation is present together with the evolved genetic background (Fig. 3). This dependency demonstrates epistatic interactions between the AnEF synonymous mutation and the evolved genetic background and strongly indicates that there are additional changes required to optimize levels of AnEF in the context of the extant *E. coli* genome. Furthermore, as shown in Fig. 4, the mRNA levels of $AnEF_{C45T}$ are higher in the evolved background compared to when moved to the ancestral

background, suggesting that epistasis within the evolved background is reinforcing EF-Tu's role as a limiting factor upon cell growth.

Upon 3,000 generations of bacterial evolution, there were seven additional nonsynonymous mutations that arose and were fixed prior to the synonymous mutation in *anEF* (genes: *mrdA*, *ydfI*, *pykF*, *ydjN*, *yfaS*, *rbsD*-[*rbsR*], and *fadA*) (Fig. 2C and D; Table S3). The mutations in *ydjN*, *fadA*, and *rbsD*-[*rbsR*] became fixed in generation 500, where YdjN functions as a L-cysteine transporter (49) and FadA and products of the *rbs* operon function in metabolism (50, 51). The genomic deletion in *rbsD*-[*rbsR*] has been observed in previous bacterial evolution experiments, in which multiple experimentally evolved populations acquired a loss in the *rbs* operon (involved in ribose catabolism) (52). This *rbs* operon deletion is hypothesized to provide an advantage in glucose minimal medium; thus, we do not suspect it is responsible for the increase in fitness associated with the AnEF synonymous mutation. Mutations fixed in generation 1,000 were in genes *mrdA*, *ydfI*, and *yfaS*. The *mrdA* gene (also known as *pbpA*) produces the protein penicillin-binding protein 2, which is responsible for maintaining antibiotic sensitivity as well as the rod cell shape in *E. coli* (53); YdfI functions in metabolism (54), while YfaS remains uncharacterized but predicted to be a part of the alpha-2-macroglobulin family (55). The final mutation to fix was in *pykF* in generation 2,500 (with *anEF*), the product of which also functions in cell metabolism (56). Changes in some of these genes, for example, *mrdA* (57) and *pykF* (58), were previously shown to increase the fitness of REL606 during laboratory evolution. How these background mutations influence AnEF remains to be explored in detail, but their occurrence in such evolution experiments using native, unaltered *E. coli* indicates that phenotypic effects of the synonymous mutation in AnEF are not causally linked on prior mutations in *mrdA*, *pykF*, or the *rbs* operon and may have arisen due to chance.

Overall, our data underscore the importance of highly expressed proteins in essential cellular processes as well as the importance of the genetic background when a synonymous substitution is favored by natural selection. The synonymous mutation in AnEF is associated with increased mRNA (Fig. 4A), increased protein (Fig. 4B), and increased polysome abundance (Fig. 6); however, population fitness is only increased when $AnEF_{C45T}$ is coupled with the evolved genetic background (Fig. 3). Taken together, these results demonstrate that synonymous mutations can be beneficial and have the potential to impact evolution when critical cellular processes are involved.

MATERIALS AND METHODS

Media and culture conditions

Liquid media are Luria-Bertani (LB; per liter, 10-g NaCl, 5-g yeast extract, and 10-g tryptone) and Davis minimal medium [25 mg/L glucose; per liter, 5.34-g K_2HPO_4, 2-g KH_2PO_4, 1-g SO_4, 0.5-g sodium citrate, 0.01% $MgSO_4$, 0.0002% thiamine (vitamin B1), and 0.0025% glucose]. Solid medium is LBA (LB with 1.5% agar) and TA (tetrazolium sugar; per liter, 10-g tryptone, 1-g yeast extract, 5-g NaCl, 1.5% agar, 10-g arabinose, and 0.005% triphenyl tetrazolium chloride). All incubations were done at 37°C. LB liquid cultures were shaken at 200 rpm for aeration, and DM25 liquid cultures were shaken at 120 rpm. All media components and chemicals were purchased from Sigma, unless noted otherwise.

Ancestral protein sequence and structure reconstruction

Ancestral protein AnEF sequence was inferred through ancestral sequence reconstruction of EF-Tu proteins as previously described (59). AnEF protein and nucleotide sequences were aligned to *E. coli* EF-Tu protein and *E. coli tufB* nucleotide sequences using MAFFT v7.490 (60). AnEF structures was predicted by LocalColabFold (61) which is a script to use AlphaFold 2.3.1 on local machines (last used April 2023). The AnEF structure was predicted using templates from PDB (*--template*), default number of prediction recycles (*--num-recycle 3*), and amber structure refinement method (*--amber*).

The predicted structure of AnEF was aligned to *E. coli* EF-Tu structure (PDB: 5AFI), and the RMSD calculation was done using UCSF Chimera MatchMaker (62). The secondary structures $anEF_{C45T}$ and *E. coli* EF-Tu mRNA regions (from −73 to +96) were predicted using mFold (63).

Strain construction

Ancestral and evolved lineages were derived from *E. coli* B strain REL606 as detailed in reference (27). The genetic marker TP22-amilCP_opt-kan-sacB-T0 was inserted in intergenic region between *rpoC* and *yjaZ* via dsDNA recombineering (28, 64, 65) to link it to the different EF-Tu alleles in strains CH6556 and CH6585 (Table S1). The genetic marker and linked EF-Tu allele were moved between strains by P1 *virA* phage-mediated transduction (28, 66). Constructs were confirmed via PCR, local Sanger DNA sequencing, and whole genome sequencing. A complete list of primers and strain genotypes is listed on Tables S1 and S2.

Experimental evolution

Experimental evolution was carried out in serial dilutions in DM25 liquid medium for 3,000 generations (~6.6 generations per day) as described previously (34) and reported for the AnEF strains (27).

Whole genome sequencing and analysis

Genomic DNA was extracted from clonal or whole population samples using DNeasy UltraClean Microbial Kit (Qiagen, 12224-50) and shipped to Microbial Genome Sequencing Center for Illumina sequencing. All Illumina sequences were analyzed for single nucleotide polymorphisms using the computational pipeline, *breseq* (67). The genomic DNA reference used was REL606 (NCBI RefSeq: NC_012967.1). The C45T synonymous mutation (i.e., V15V) was confirmed with Oxford Nanopore sequencing as well. The quality of Nanopore sequences was checked using fastqc v0.12.1 (68). The reads having base quality lower than 20 were trimmed with Nanofilt v2.8.0 (69) using parameters *-q 20 –headcrop 50*. Trimmed sequences were aligned to the reference genome REL606 (NCBI RefSeq: NC_012967.1) with minimap2 v2.26 (70). The "sam" files that resulted from alignment were converted into "bam" files and sorted using samtools v1.3.1 (71). The variants were called using NanoCaller v3.0.0 (72). The variants were annotated using vcf-annotator 0.7 (73).

RNA extractions, cDNA synthesis, and quantitative PCR

Strains were grown in LB medium and collected at 0.3–0.6 OD_{600} for RNA extraction. Pellets were lysed and prepared following the standard protocol in Rneasy kit (Qiagen, 74104). Following RNA extraction, samples were removed of any contaminating genomic DNA using the DNase I standard protocol (Invitrogen, 18068015). Following DNase treatment, RNA extracts were synthesized into cDNA using reverse transcriptase SuperScript IV First-Strand Synthesis System (Invitrogen, 18091050). Finally, all cDNA samples were run on PCR to confirm no genomic DNA contamination before quantitative PCR. All cDNA samples (three biological replicates) were run in SsoAdvanced Universal SYBR Green Supermix (Bio-Rad, 1725271) in three technical replicates for 40 cycles. All primers are listed on Table S2. ΔΔCq values were calculated using housekeeping gene *rpoB* as a control.

Immunoblotting experiments

Strains were grown in LB-rich medium and collected at 0.3–0.6 OD_{600} for cell lysis (three biological replicates). Cell pellets were lysed in 300 µL of lysis buffer [10-mL BugBuster (Millipore 70584-4), ¼ tablet cOmplete Protease Inhibitor Cocktail EDTA-Free (Roche)] for 20 min at room temperature and centrifuged at 13,000 rpm at 4°C for 30 min to

clear all cell debris. Protein concentrations were measured using BCA assay (Thermo Fisher 23227) and stored at −20°C. Whole cell lysates were linearized at 95°C for 5 min and were run on a 12% resolving Tris-glycine SDS-PAGE gel at a constant voltage of 125 V. Protein bands were then transferred to a nitrocellulose membrane at a constant amperage of 400 mA for 45 min. All membranes were blocked with 5% nonfat milk for 1 hour at room temperature. To visualize EF-Tu bands, membranes were probed with 1:1,000 EF-Tu monoclonal antibody (Hycult Biotech mAb 900; catalog no. HM6010) for at 4°C overnight, followed by incubation with 1:10,000 IRDye 680RD anti-mouse secondary antibody (LI-COR, 929-70050) for 1 hour at room temperature. All membranes were imaged using the LI-COR Odyssey XF. To normalize for band quantitation, membranes were stained with GelCode Blue Stain (Thermo Fisher, 24590) for 5 min and destained for 10 min using a destaining solution composed of 40% dH_20, 10% acetic acid, and 50% methanol. Bands were quantified using ImageJ, and statistics were calculated using Rstudio.

Fitness assays

All competition assays were followed per published Ara–/+ competition protocol (34). Mixed populations were revived with 100 µL from a glycerol stock into 10 mL of LB medium and grown overnight shaking at 250 rpm at 37°C. Clonal populations were revived with 2 µL from a glycerol stock. The next day, each mixed population or clonal strain was preconditioned by diluting 1:10,000 in 10 mL of DM25 medium (five replicates each) and grown overnight shaking at 250 rpm at 37°C. To begin the competition, two selected strains were combined in equal amounts (50 µL) into 10 mL of DM25, plated 100× diluted on TA agar (d_0), and grown for 24 hours shaking at 250 rpm at 37°C. After 24 hours, the competition assay was plated 100× diluted on TA agar a second time (d_1) and grown at 37°C overnight. All plates were imaged after 24 hours. To calculate relative fitness (W), we calculated the ratio of each strain's Malthusian parameters (M_A and M_B) as follows:

$$M_A = ln(100^*Ad_0)/Ad_1$$
$$M_B = ln(100^*Bd_0)/Bd_1$$
$$W = M_A/M_B$$

Polysome profiling

Samples were prepped in accordance with Qin and Frederick (74). Each strain was grown to mid-log (OD_{600} 0.3–0.6) at 37°C and shaking at 200 rpm for a total of six biological replicates and two technical replicates. At mid-log, 35 mL of culture was collected, pelleted at 4,000 rpm at 4°C for 5 minutes, resuspended in 500 µL of chilled lysis buffer (10 mM Tris-HCl pH 8.0, 10 mM $MgCl_2$, 1 mg/mL lysozyme), and flash frozen in liquid nitrogen. The lysates were then thawed in ice water and immediately refrozen in liquid nitrogen and stored at −80°C. To separate polysomes, lysates were thawed on ice and resuspended with 15 µL of 10% sodium deoxycholate. The lysates were then cleared of cell debris at 10,000 rpm at 4°C for 10 min. A normalized volume of 500,000 ng of RNA was carefully loaded on top a sucrose gradient (10%–40% sucrose, 20 mM Tris-HCl pH 8.0, 10 mM $MgCl_2$, 100 mM NH_4Cl, 2 mM DTT, assembled using Biocomp Gradient Master) and ultracentrifuged (Beckman Coulter Optima XE-90, Rotor SW41Ti) for 3 hours at 35,000 rpm at 4°C. To collect polysome profiles, samples were collected, and RNA was measured at 260 nm using the Biocomp scanner; the overall assay was repeated twice. Ribosome abundance was measured by calculating the area under the curve (AUC) for peaks corresponding to the 30S subunit, 50S subunit, 70S monosome, and polysomes comprising two to four ribosomes. Subsequently, peak areas were normalized by the total area under the curve (30S + 50S + 70S + polysomes). Areas under the curve were generated by averaging across both trials.

Statistical tests

Data analysis was done using Rstudio, ImageJ, and Excel. All data replicates were tested for statistical significance using paired, two-tailed *t*-tests and ANOVA unless stated otherwise.

ACKNOWLEDGMENTS

The authors would like to thank Aude Trinquier and Bruno Cuevas-Zuviria and the members of the Kacar Lab for valuable feedback.

This work was supported by a grant from the National Institutes of Health, USA (NIH #T32GM136536), and a NASA Early Career Collaboration Award (K.M.), UW Foundation Hiroshi and Sugiyama Fund for Graduate Studies (E.F.), and the John Templeton Foundation (#61926).

Conceptualized the study: K.M. and B.K.; performed experiments: K.M., S.R., E.F., E.G., A.H., B.K.; sequence, structure, and computational analyses: K.M. and E.F.; wrote the paper: K.M. and B.K.; edited and reviewed: all authors; final version approved by all authors.

AUTHOR AFFILIATIONS

[1]Department of Bacteriology, University of Wisconsin-Madison, Madison, Wisconsin, USA
[2]Department of Molecular and Cellular Biology, University of Arizona, Tucson, Arizona, USA
[3]School of Plant Sciences, University of Arizona, Tucson, Arizona, USA
[4]Microbial Doctoral Training Program, University of Wisconsin-Madison, Madison, Wisconsin, USA
[5]Department of Medical Biochemistry and Microbiology, Uppsala University, Uppsala, Sweden

AUTHOR ORCIDs

Kaitlyn M. McGrath http://orcid.org/0000-0002-3151-0439
Steven J. Russell http://orcid.org/0000-0002-5420-2092
Evrim Fer http://orcid.org/0000-0003-2731-1207
Eva Garmendia http://orcid.org/0000-0003-0382-0234
David A. Baltrus http://orcid.org/0000-0002-5166-9551
Betül Kaçar http://orcid.org/0000-0002-0482-2357

FUNDING

Funder	Grant(s)	Author(s)
HHS | National Institutes of Health (NIH)	T32GM136536	Kaitlyn M. McGrath
John Templeton Foundation (JTF)	61926	Kaitlyn M. McGrath Steven J. Russell Evrim Fer Ali Hosgel Betül Kaçar
NASA | NASA Astrobiology Institute (NAI)		Kaitlyn M. McGrath Betül Kaçar
University of Wisconsin Foundation (UW Foundation)		Evrim Fer

AUTHOR CONTRIBUTIONS

Kaitlyn M. McGrath, Conceptualization, Data curation, Formal analysis, Investigation, Methodology, Validation, Visualization, Writing – original draft, Writing – review and editing | Steven J. Russell, Data curation, Formal analysis, Investigation, Methodology, Visualization, Writing – review and editing | Evrim Fer, Data curation, Formal analysis, Investigation, Methodology, Visualization, Writing – review and editing | Eva Garmendia, Methodology, Validation, Writing – review and editing | Ali Hosgel, Data curation, Validation | David A. Baltrus, Formal analysis, Writing – review and editing.

DATA AVAILABILITY

All raw data are available on GitHub (https://github.com/kacarlab/EFTUSyn). All sequences are available under NCBI BioProject number PRJNA1052091.

ADDITIONAL FILES

The following material is available online.

Supplemental Material

Supplemental material (JB00329-23-s0001.docx). Tables S1 to S3; Figures S1 to S4.

REFERENCES

1. Berger EM. 1977. Are synonymous mutations adaptively neutral. American Natur 111:606–607. https://doi.org/10.1086/283192
2. Post LE, Nomura M. 1980. DNA sequences from the STR operon of *Escherichia coli*. J Biological Chem 255:4660–4666. https://doi.org/10.1016/S0021-9258(19)85545-X
3. Gouy M, Gautier C. 1982. Codon usage in bacteria: correlation with gene expressivity. Nucleic Acids Res 10:7055–7074. https://doi.org/10.1093/nar/10.22.7055
4. Qin H, Wu WB, Comeron JM, Kreitman M, Li WH. 2004. Intragenic spatial patterns of codon usage bias in prokaryotic and eukaryotic genomes. Genetics 168:2245–2260. https://doi.org/10.1534/genetics.104.030866
5. Hershberg R, Petrov DA. 2008. Selection on codon bias. Annu Rev Genet 42:287–299. https://doi.org/10.1146/annurev.genet.42.110807.091442
6. Bailey SF, Hinz A, Kassen R. 2014. Adaptive synonymous mutations in an experimentally evolved *Pseudomonas fluorescens* population. Nat Commun 5:4076. https://doi.org/10.1038/ncomms5076
7. Bailey SF, Alonso Morales LA, Kassen R. 2021. Effects of synonymous mutations beyond codon bias: the evidence for adaptive synonymous substitutions from microbial evolution experiments. Genome Biol Evol 13:evab141. https://doi.org/10.1093/gbe/evab141
8. Kershner JP, Yu McLoughlin S, Kim J, Morgenthaler A, Ebmeier CC, Old WM, Copley SD. 2016. A synonymous mutation upstream of the gene encoding a weak-link enzyme causes an ultrasensitive response in growth rate. J Bacteriol 198:2853–2863. https://doi.org/10.1128/JB.00262-16
9. Knöppel A, Näsvall J, Andersson DI. 2016. Compensating the fitness costs of synonymous mutations. Mol Biol Evol 33:1461–1477. https://doi.org/10.1093/molbev/msw028
10. Kristofich J, Morgenthaler AB, Kinney WR, Ebmeier CC, Snyder DJ, Old WM, Cooper VS, Copley SD, Matic I. 2018. Synonymous mutations make dramatic contributions to fitness when growth is limited by a weak-link enzyme. PLoS Genet 14:e1007615. https://doi.org/10.1371/journal.pgen.1007615
11. Chamary JV, Hurst LD. 2005. Evidence for selection on synonymous mutations affecting stability of mRNA secondary structure in mammals. Genome Biol 6:R75. https://doi.org/10.1186/gb-2005-6-9-r75
12. Shabalina SA, Ogurtsov AY, Spiridonov NA. 2006. A periodic pattern of mRNA secondary structure created by the genetic code. Nucleic Acids Res 34:2428–2437. https://doi.org/10.1093/nar/gkl287
13. Lind PA, Andersson DI. 2013. Fitness costs of synonymous mutations in the Rpst gene can be compensated by restoring mRNA base pairing. PLoS One 8:e63373. https://doi.org/10.1371/journal.pone.0063373
14. Cannarozzi G, Schraudolph NN, Faty M, von Rohr P, Friberg MT, Roth AC, Gonnet P, Gonnet G, Barral Y. 2010. A role for codon order in translation dynamics. Cell 141:355–367. https://doi.org/10.1016/j.cell.2010.02.036
15. Kramer EB, Farabaugh PJ. 2007. The frequency of translational misreading errors in *E. coli* is largely determined by Trna competition. RNA 13:87–96. https://doi.org/10.1261/rna.294907
16. Stoletzki N, Eyre-Walker A. 2007. Synonymous codon usage in *Escherichia coli:* selection for translational accuracy. Mol Biol Evol 24:374–381. https://doi.org/10.1093/molbev/msl166
17. Yu CH, Dang Y, Zhou Z, Wu C, Zhao F, Sachs MS, Liu Y. 2015. Codon usage influences the local rate of translation elongation to regulate co-translational protein folding. Mol Cell 59:744–754. https://doi.org/10.1016/j.molcel.2015.07.018
18. Oh E, Becker AH, Sandikci A, Huber D, Chaba R, Gloge F, Nichols RJ, Typas A, Gross CA, Kramer G, Weissman JS, Bukau B. 2011. Selective ribosome profiling reveals the cotranslational chaperone action of trigger factor *in vivo*. Cell 147:1295–1308. https://doi.org/10.1016/j.cell.2011.10.044
19. Plotkin JB, Kudla G. 2011. Synonymous but not the same: the causes and consequences of codon bias. Nat Rev Genet 12:32–42. https://doi.org/10.1038/nrg2899
20. Bulmer M. 1991. The selection-mutation-drift theory of synonymous codon usage. Genetics 129:897–907. https://doi.org/10.1093/genetics/129.3.897
21. Sharp PM, Bailes E, Grocock RJ, Peden JF, Sockett RE. 2005. Variation in the strength of selected codon usage bias among bacteria. Nucleic Acids Res 33:1141–1153. https://doi.org/10.1093/nar/gki242
22. Drummond DA, Wilke CO. 2008. Mistranslation-induced protein misfolding as a dominant constraint on coding-sequence evolution. Cell 134:341–352. https://doi.org/10.1016/j.cell.2008.05.042
23. Zhou T, Weems M, Wilke CO. 2009. Translationally optimal codons associate with structurally sensitive sites in proteins. Mol Biol Evol 26:1571–1580. https://doi.org/10.1093/molbev/msp070
24. Agashe D, Martinez-Gomez NC, Drummond DA, Marx CJ. 2013. Good codons, bad transcript: large reductions in gene expression and fitness arising from synonymous mutations in a key enzyme. Mol Biol Evol 30:549–560. https://doi.org/10.1093/molbev/mss273
25. Lind PA, Berg OG, Andersson DI. 2010. Mutational robustness of ribosomal protein genes. Science 330:825–827. https://doi.org/10.1126/science.1194617
26. Lebeuf-Taylor E, McCloskey N, Bailey SF, Hinz A, Kassen R. 2019. The distribution of fitness effects among synonymous mutations in a gene

under directional selection. Elife 8:e45952. https://doi.org/10.7554/eLife.45952
27. Kacar B, Ge X, Sanyal S, Gaucher EA. 2017. Experimental evolution of *Escherichia coli* harboring an ancient translation protein. J Mol Evol 84:69–84. https://doi.org/10.1007/s00239-017-9781-0
28. Kacar B, Garmendia E, Tuncbag N, Andersson DI, Hughes D, Laub MT, Levin B, Rainey P. 2017. Functional constraints on replacing an essential gene with its ancient and modern homologs. mBio 8. https://doi.org/10.1128/mBio.01276-17
29. Nissen P, Kjeldgaard M, Thirup S, Polekhina G, Reshetnikova L, Clark BF, Nyborg J. 1995. Crystal structure of the ternary complex of PhetRNAphe, EF-Tu, and a GTP analog. Science 270:1464–1472. https://doi.org/10.1126/science.270.5241.1464
30. Wohlgemuth I, Pohl C, Mittelstaet J, Konevega AL, Rodnina MV. 2011. Evolutionary optimization of speed and accuracy of decoding on the ribosome. Philos Trans R Soc Lond B Biol Sci 366:2979–2986. https://doi.org/10.1098/rstb.2011.0138
31. Furano AV. 1975. Content of elongation factor Tu in *Escherichia coli*. Proc Natl Acad Sci U S A 72:4780–4784. https://doi.org/10.1073/pnas.72.12.4780
32. Harvey KL, Jarocki VM, Charles IG, Djordjevic SP. 2019. The diverse functional roles of elongation factor Tu (EF-Tu) in microbial pathogenesis. Front Microbiol 10:2351. https://doi.org/10.3389/fmicb.2019.02351
33. Fischer N, Neumann P, Konevega AL, Bock LV, Ficner R, Rodnina MV, Stark H. 2015. Structure of the *E. coli* ribosome–EF-Tu complex at <3 Å resolution by C_S-corrected cryo-EM. Nature 520:567–570. https://doi.org/10.1038/nature14275
34. Elena SF, Lenski RE. 2003. Evolution experiments with microorganisms: the dynamics and genetic bases of adaptation. Nat Rev Genet 4:457–469. https://doi.org/10.1038/nrg1088
35. Kjeldgaard NO, Kurland CG. 1963. The distribution of soluble and ribosomal RNA as a function of growth rate. J Mole Biol 6:341–348. https://doi.org/10.1016/S0022-2836(63)80093-5
36. EckerRE, SchaechterM. 1963. Ribosome content and the rate of growth of *Salmonella typhimurium*. Biochim Biophys Acta 76:275–279. https://doi.org/10.1016/0926-6550(63)90040-9
37. Scott M, Klumpp S, Mateescu EM, Hwa T. 2014. Emergence of robust growth laws from optimal regulation of ribosome synthesis. Mol Syst Biol 10:747. https://doi.org/10.15252/msb.20145379
38. Dai X, Zhu M, Warren M, Balakrishnan R, Patsalo V, Okano H, Williamson JR, Fredrick K, Wang Y-P, Hwa T. 2016. Reduction of translating ribosomes enables *Escherichia coli* to maintain elongation rates during slow growth. Nat Microbiol 2:16231. https://doi.org/10.1038/nmicrobiol.2016.231
39. Pedersen S, Bloch PL, Reeh S, Neidhardt FC. 1978. Patterns of protein synthesis in *E. coli*: a catalog of the amount of 140 individual proteins at different growth rates. Cell 14:179–190. https://doi.org/10.1016/0092-8674(78)90312-4
40. Lucas-Lenard J, Lipmann F. 1971. Protein biosynthesis. Annu Rev Biochem 40:409–448. https://doi.org/10.1146/annurev.bi.40.070171.002205
41. Ramakrishnan V. 2002. Ribosome structure and the mechanism of translation. Cell 108:557–572. https://doi.org/10.1016/S0092-8674(02)00619-0
42. Rodnina MV. 2018. Translation in prokaryotes. Cold Spring Harb Perspect Biol 10:a032664. https://doi.org/10.1101/cshperspect.a032664
43. Venkataram S, Monasky R, Sikaroodi SH, Kryazhimskiy S, Kacar B. 2020. Evolutionary stalling and a limit on the power of natural selection to improve a cellular module. Proc Natl Acad Sci U S A 117:18582–18590. https://doi.org/10.1073/pnas.1921881117
44. Agashe D, Sane M, Phalnikar K, Diwan GD, Habibullah A, Martinez-Gomez NC, Sahasrabuddhe V, Polachek W, Wang J, Chubiz LM, Marx CJ. 2016. Large-effect beneficial synonymous mutations mediate rapid and parallel adaptation in a bacterium. Mol Biol Evol 33:1542–1553. https://doi.org/10.1093/molbev/msw035
45. Zwart MP, Schenk MF, Hwang S, Koopmanschap B, de Lange N, van de Pol L, Nga TTT, Szendro IG, Krug J, de Visser JAGM. 2018. Unraveling the causes of adaptive benefits of synonymous mutations in TEM-1 β-lactamase. Heredity (Edinb) 121:406–421. https://doi.org/10.1038/s41437-018-0104-z
46. Brandis G, Bergman JM, Hughes D. 2016. Autoregulation of the *tufB* operon in *Salmonella*. Mol Microbiol 100:1004–1016. https://doi.org/10.1111/mmi.13364
47. Hénaut A, Danchin A. 1996. Analysis and predictions from *Escherichia coli* sequences, or *E. coli in silico*. *Escherichia coli* and *Salmonella*. Cell Mol Biol:2047–2066.
48. De Tarafder A, Parajuli NP, Majumdar S, Kaçar B, Sanyal S. 2021. Kinetic analysis suggests evolution of ribosome specificity in modern elongation factor-tus from "generalist" ancestors. Mol Biol Evol 38:3436–3444. https://doi.org/10.1093/molbev/msab114
49. Ohtsu I, Kawano Y, Suzuki M, Morigasaki S, Saiki K, Yamazaki S, Nonaka G, Takagi H. 2015. Uptake of L-cystine via an ABC transporter contributes defense of oxidative stress in the L-cystine export-dependent manner in *Escherichia coli*. PLoS One 10:e0120619. https://doi.org/10.1371/journal.pone.0120619
50. Pawar S, Schulz H. 1981. The structure of the multienzyme complex of fatty acid oxidation from *Escherichia coli*. J Biol Chem 256:3894–3899.
51. David J, Wiesmeyer H. 1970. Regulation of ribose metabolism in *Escherichia coli*. I. The ribose catabolic pathway. Biochim Biophys Acta 208:45–55. https://doi.org/10.1016/0304-4165(70)90047-4
52. Cooper VS, Schneider D, Blot M, Lenski RE. 2001. Mechanisms causing rapid and parallel losses of ribose catabolism in evolving populations of *Escherichia coli* B. J Bacteriol 183:2834–2841. https://doi.org/10.1128/JB.183.9.2834-2841.2001
53. Begg KJ, Donachie WD. 1998. Division planes alternate in spherical cells of *Escherichia coli*. J Bacteriol 180:2564–2567. https://doi.org/10.1128/JB.180.9.2564-2567.1998
54. Da Re S, Valle J, Charbonnel N, Beloin C, Latour-Lambert P, Faure P, Turlin E, Le Bouguénec C, Renauld-Mongénie G, Forestier C, Ghigo J-M. 2013. Identification of commensal *Escherichia coli* genes involved in biofilm resistance to pathogen colonization. PLoS One 8:e61628. https://doi.org/10.1371/journal.pone.0061628
55. El Khoury JY, Maure A, Gingras H, Leprohon P, Ouellette M, Bulman Z. 2019. Chemogenomic screen for imipenem resistance in gram-negative bacteria. mSystems 4:e00465-19. https://doi.org/10.1128/mSystems.00465-19
56. Ponce E, Flores N, Martinez A, Valle F, Bolívar F. 1995. Cloning of the two pyruvate kinase isoenzyme structural genes from *Escherichia coli:* the relative roles of these enzymes in pyruvate biosynthesis. J Bacteriol 177:5719–5722. https://doi.org/10.1128/jb.177.19.5719-5722.1995
57. Philippe N, Pelosi L, Lenski RE, Schneider D. 2009. Evolution of penicillin-binding protein 2 concentration and cell shape during a long-term experiment with *Escherichia coli*. J Bacteriol 191:909–921. https://doi.org/10.1128/JB.01419-08
58. Peng F, Widmann S, Wünsche A, Duan K, Donovan KA, Dobson RCJ, Lenski RE, Cooper TF. 2018. Effects of beneficial mutations in Pykf gene vary over time and across replicate populations in a long-term experiment with bacteria. Mol Biol Evol 35:202–210. https://doi.org/10.1093/molbev/msx279
59. Kaçar B, Gaucher E. 2012. Towards the recapitulation of ancient history in the laboratory: combining synthetic biology with experimental evolution Artificial life XIII: proceedings of the thirteenth international conference on the synthesis and simulation of living systems, p 11–18. https://doi.org/10.48550/arXiv.1209.5032
60. Katoh K, Misawa K, Kuma K, Miyata T. 2002. MAFFT: a novel method for rapid multiple sequence alignment based on fast fourier transform. Nucleic Acids Res 30:3059–3066. https://doi.org/10.1093/nar/gkf436
61. Mirdita M, Schütze K, Moriwaki Y, Heo L, Ovchinnikov S, Steinegger M. 2022. Colabfold: making protein folding accessible to all. Nat Methods 19:679–682. https://doi.org/10.1038/s41592-022-01488-1
62. Meng EC, Pettersen EF, Couch GS, Huang CC, Ferrin TE. 2006. Tools for integrated sequence-structure analysis with UCSF chimera. BMC Bioinformatics 7:339. https://doi.org/10.1186/1471-2105-7-339
63. Zuker M. 2003. Mfold web server for nucleic acid folding and hybridization prediction. Nucleic Acids Res 31:3406–3415. https://doi.org/10.1093/nar/gkg595
64. Datsenko KA, Wanner BL. 2000. One-step inactivation of chromosomal genes in *Escherichia coli* K-12 using PCR products. Proc Natl Acad Sci U S A 97:6640–6645. https://doi.org/10.1073/pnas.120163297
65. Yu D, Ellis HM, Lee EC, Jenkins NA, Copeland NG, Court DL. 2000. An efficient recombination system for chromosome engineering in

Escherichia coli. Proc Natl Acad Sci U S A 97:5978–5983. https://doi.org/10.1073/pnas.100127597
66. Schmieger H, Backhaus H. 1973. The origin of DNA in transducing particles in P22-mutants with increased transduction-frequencies (Ht-mutants). Mol Gen Genet 120:181–190. https://doi.org/10.1007/BF00267246
67. Deatherage DE, Barrick JE. 2014. Identification of mutations in laboratory-evolved microbes from next-generation sequencing data using *breseq*. Methods Mol Biol 1151:165–188. https://doi.org/10.1007/978-1-4939-0554-6_12
68. Andrews S. 2010. FastQC: a quality control tool for high throughput sequence data. Babraham Bioinformatics 10:f1000research.
69. De Coster W, D'Hert S, Schultz DT, Cruts M, Van Broeckhoven C. 2018. Nanopack: visualizing and processing long-read sequencing data. Bioinformatics 34:2666–2669. https://doi.org/10.1093/bioinformatics/bty149
70. Li H. 2018. Minimap2: pairwise alignment for nucleotide sequences. Bioinformatics 34:3094–3100. https://doi.org/10.1093/bioinformatics/bty191
71. Li H, Handsaker B, Wysoker A, Fennell T, Ruan J, Homer N, Marth G, Abecasis G, Durbin R, 1000 Genome Project Data Processing Subgroup. 2009. The sequence alignment/map format and samtools. Bioinformatics 25:2078–2079. https://doi.org/10.1093/bioinformatics/btp352
72. Ahsan MU, Liu Q, Fang L, Wang K. 2021. Nanocaller for accurate detection of SNPs and Indels in difficult-to-map regions from long-read sequencing by haplotype-aware deep neural networks. Genome Biol 22:261. https://doi.org/10.1186/s13059-021-02472-2
73. Petit RA. 2010. Vcf-annotator., Github, v0.7, May 2023.
74. Qin D, Fredrick K. 2013. Analysis of polysomes from bacteria. Methods Enzymol 530:159–172. https://doi.org/10.1016/B978-0-12-420037-1.00008-7